fortune Journals

Research Article

JOURNAL OF RADIOLOGY AND CLINICAL IMAGING

ISSN: 2644-2809

Longitudinal Single Neuron Electrophysiology in the Mouse Visual Cortex using Microwire Brush Arrays

Alireza Saeedi[1,2], Kun Wang[1,3], Nikos K. Logothetis[1,3,4], Masataka Watanabe[1,5,*].

Abstract

Long-term stable single-unit recording in the brain is essential to the longitudinal study of brain functions. Microwire brush arrays (MBA) compliant with brain tissue are excellent tools for long-term stable neural recordings. However, there are multiple challenges in applying these electrodes to small animals (e.g., mice). Here, we resolve several challenges of using MBA probes in the mouse. By integrating microwire electrodes and ultra-light microdrives, we performed long-term electrophysiology and tracked the same neuronal population in the mouse visual cortex over two months. Moreover, we found that the orientation-tuning properties of visual neurons remain unchanged and used the visual response fingerprint of the neurons to track them over days of recording. Furthermore, we propose the use of Nonclassical Multidimensional Scaling (MDS) for inferring microwires' spatial organization in the brain and demonstrate its successful use in spatiotemporal template matching algorithms for spike sorting.

Keywords: Long-term Electrophysiology; Microwire Brush Electrodes; Mouse Visual Cortex; Stable Selectivity

Introduction

Tracking single-unit activity in the brain is crucial to the longitudinal study of brain functions. Implantable neural electrodes are one of the most common tools for recording single-unit activity in the brain [1-9]. However, the quality of the recorded signal decreases over time due to chronic tissue reaction and loss of neurons around the tip of recording sites [9-15]. Therefore, maintaining high-quality chronic electrophysiological recordings remains a critical challenge in longitudinal studies of brain functions and developing neural prosthetics. Flexible neural probes are known to reduce relative shear motion and improve the stability of neuronal interfaces as they are compliant with brain tissue [16-27]. Microwire bundle electrodes are one of the most flexible neural probes, which allow tracking of single-unit activities over a long period. For instance, McMahon et al. have successfully tracked the activities of neurons in monkeys' visual cortex over months [7]. However, these probes are susceptible to over-bending during insertion into the brain. Several studies have addressed this matter, and different techniques have been developed to increase their stiffness during insertion into the brain [9, 28]. Another monkey study used microdrives to slowly insert the probe into the brain tissue to prevent over-bending of the wires [7]. Another challenge of using MBA probes is spike clustering and single-unit isolation. New spike sorting methods use the spatiotemporal template matching technique [29], which requires the spatial organization of recording sites in the brain (i. e., channel map). Since the channel map in MBA probes is unknown due to its unpredictable

Affiliation:

[1]Department of Physiology of Cognitive Processes, Max Planck Institute for Biological Cybernetics, 72076 Tübingen, Germany

[2]Research Group Neurobiology of Magnetoreception, Max Planck Institute for Neurobiology of Behavior – caesar, 53175, Bonn, Germany

[3]Department of Physiology of Cognitive Processes, International Center for Primate Brain Research, Songjiang District, Shanghai201602, China

[4]Centre for Imaging Sciences, University of Manchester, Manchester M139PT, UK

[5]Department of Systems Innovation, School of Engineering, the University of Tokyo, Tokyo, Japan

Corresponding author:
Masataka Watanabe. Department of Physiology of Cognitive Processes, Max Planck Institute for Biological Cybernetics, 72076 Tübingen, Germany; Department of Systems Innovation, School of Engineering, the University of Tokyo, Tokyo, Japan.

Citation: Alireza Saeedi, Kun Wang, Nikos K. Logothetis, Masataka Watanabe. Longitudinal Single Neuron Electrophysiology in the Mouse Visual Cortex using Microwire Brush Arrays. Journal of Radiology and Clinical Imaging 7 (2024): 09-19.

Received: November 29, 2023
Accepted: December 08, 2023
Published: May 16, 2024

spread in neural tissue, the post-processing and spike sorting of recorded data requires extra considerations. This study combines commercially available microwire electrodes with an ultra-light in-house microdrive to record from the mouse visual cortex. We use Nonclassical Multidimensional Scaling (MDS) to infer the spatial organization of microwires in the brain for further spike sorting with the Kilosort algorithm [29]. We successfully tracked the activities of visually evoked neurons for ten weeks and demonstrated that their orientation and direction-tuning properties remain unchanged.

Methods and Materials

Subjects

We implanted two microwire bundle electrodes into the primary visual cortex (V1) of two mice (C57BL/6, male). As the objective of this study is to develop an electrophysiological recording technique, which is less likely to be significantly influenced by gender, we did not specifically select a particular sex for our study. All animal procedures were approved by the local authorities at the Max Planck Institute and University of Tübingen and in compliance with EU Directive 2010/63/EU (European Community Guidelines for the Care and Use of Laboratory Animals).

Apparatus

We used two microwire brush arrays (MBA) with 16 or 32 microwires (12.5 µm diameter, Platinum/Iridium alloy, commercially available at MicroProbes, MA). The wires were insulated with a polyimide microfil tube with a length of 9 mm and an outer diameter of 350 µm. At the tip of the electrodes, the length of wires extended beyond the microfil tube was 1.5 mm. The tail of wires was extended into a flexible output cable of a length of 25 mm and connected to male Omnetics connectors (A79014-001, 16 channels, 18 pins; A79022-001, 32 channels, 36 pins). Two extra silver wires were connected to the connector as a reference and ground cable. The MBA electrodes were combined with an ultra-light in-house microdrive to slowly advance the probe into brain tissue and prevent the over-bending of wires during the insertion procedure (Figure 1a). The microdrive size was 11x3x2 mm with six mm of traveling distance and 0.22 g of weight. The thread pitch was 250 µm. The microdrive consists of two plastic plates, one movable and one fixed. A sharpened stainless-steel tube (outer diameter of 0.6 mm and length of 0.5 mm) was connected to the lower surface of the fixed plate to function as a guide tube in the insertion procedure. The microfil tube was glued to the movable plate so that it could move up and down with the movable plate.

Surgical Procedures

Anesthesia procedures were started by inducing 2.5 % of isoflurane and were maintained during surgery by 1-2 %. Furthermore, Atropine (Atropinsulfat B. Braun, 0.3mg/kg) and Buprenorphine (0.1 mg/kg) were injected subcutaneously to reduce bronchial secretions and as analgesics, respectively. The scalp was sterilized, and an incision was made to expose the bregma and lambda sutures. A lightweight head-post was attached to the skull using an adhesive primer and dental cement (Tetric EvoFlow dental cement, Ivoclar Vivadent; OptiBond FL primer and adhesive, Kerr dental). A well was made around the exposed site using dental cement. Then a tiny craniotomy window (1.5 mm^2) was opened above the V1 at 2.5 mm laterally from the midline and 4 mm posterior to the bregma over the left hemisphere. The MBA electrode with microdrive was implanted vertically into the brain. At the time of implantation, the tip of the wires was inside the guide tube, while the entrance of the guide tube was coated with PEG 4000 [9] to prevent entering brain tissue into it. After implantation, the lower plate of the drive was fixed to the skull using dental cement. Two silver wires were installed under the skull and above the dura around the frontal lobe as references and ground for extracellular recordings. A protective cap with copper mesh was built and fixed to the well with dental cement, and the Omnetics connector was attached to the inner part of the cap using dental cement (Figure1b top). During the recovery period, Flunixin (4mg/kg) administration continued every 12 hours as an analgesic for three days, and antibiotics (Baytril, 5mg/kg) administration continued every 24 hours for five days. The five days of recovery were followed by three days (0.5 hours/day) of habituation to the experimental setup and head- fixation. Moreover, during the habituation days, electrodes were lowered slowly into the brain using the Microdrive (twice a day and each time about 125 µm). Electrophysiological recording started after habituation and continued for 4 or 10 weeks. After weeks of recording, mice were euthanized, and the electrode was extracted (Figure 1b bottom).

Electrophysiological Recording Procedure

After the habituation, electrophysiological recordings were started. For mouse #1, in which we implanted a 16-channel electrode, the recording continued for four weeks, and for mouse #2 with a 32-channel electrode, the recording continued for ten weeks. Overall, we had 26 days of recording for each mouse in the mentioned period. The electrophysiology recordings (one hour a day) were done on the head-fixed mice in a dark and isolated room while they were allowed to sit or run on a disk. The electrophysiological activities were captured by the MBA electrodes. The signal was then amplified and digitized at 30 kHz by a headstage pre-amplifier (Intan RHD2000 headstage or Blackrock CrePlex M headstage) and transferred to the RHD recording system (Intan Technologies) or Cerebus data acquisition system (Blackrock Microsystems LLC). An example of high-pass filtered data is shown in Figure 1c. The recording duration on each recording day was one hour. At the end of each recording day, the mice were put back in the animal facility.

Saeedi A, et al., J Radiol Clin Imaging 2024
DOI:10.26502/jrci.2809091

Visual stimulation and experimental design

For mouse #1, we recorded only spontaneous activities of neurons. For mouse # 2, we presented visual stimuli during the recording. We projected stimuli onto a gamma-corrected LED monitor (Dell U2412M, 24 inches, 60 Hz) using MATLAB (MathWorks, Inc.) and Psychophysics Toolbox Version 3 (PTB-3). Moreover, the monitor was placed 20 cm in front of the animal's right eye. A small white square was always presented simultaneously with the main stimulus at the lower right corner of the monitor to capture the stimulus onset time using an in-house built photodiode sensor. The first recording session was receptive field (RF) mapping to capture the receptive field of neurons near electrode sites and ensure the RF of all the channels falls into the monitor (Figure1d). For RF mapping, we presented black squares (8° widths) in different locations of 8 by 13 grids on a gray background. The presentation duration for each square was 100 ms, and the inter-stimulus interval was 100 ms. The total duration of the RF mapping session was 20 minutes. After this session, we extracted multi-unit activity (MUA) in response to each square by a band-pass filter (140-1000 Hz) and detected stimulus onsets using the photodiode. The duration of the MUA analysis was 10 minutes. A direction tuning session followed this, where we presented full screen drifting grating (temporal frequency 3 Hz, spatial frequency 0.05 cycles/ degree) and eight drifting directions (from 0° to 315° with 45° steps). The duration of each stimulus presentation was 600 ms, and the inter-stimulus interval was 500 ms. Each stimulus direction was presented for 120 trials; the whole session was 20 minutes long. Figure 1e summarizes the experimental procedure of the current study, and Figure 1f illustrates a schematic representation of the electrophysiology setup.

Post-processing data analysis

To capture spike time and clustering, we concatenated the recorded data in all recording days for each mouse. To estimate the location of wire tips in the brain and the channel map of implanted electrodes, we used the MDS method, which estimates the coordinates points using the dissimilarity matrix [30]. For this purpose, first, we extract the MUA signal by applying a band-pass filter (300-7000 Hz). Next, we calculated the cross-correlation matrix (Figure 1g) between all the channels and the dissimilarity Matrix as D=1-C. Where D is the dissimilarity matrix and C is the correlation matrix. We next used Matlab's built-in function (mdscale) to implement MDS and estimate the channel map. Figure 1h shows the estimation of relative location of wires mapped on a 2-dimental space. We fed the concatenated data and the estimated channel map to the Kilosort algorithm with the default parameters [29, 31, 32]. Kilosort is a fast and accurate semi-automatic spike sorting algorithm with batch-based optimization running on GPUs and a post-clustering merging step. Moreover, it resolves the electrode drift problem and can properly track the same neurons for long-term recording [32]. To relabel the identified clusters and further merging and splitting of clusters, we performed a manual clustering using template-GUI [33,34]. The Kilosort is a template-matching algorithm that fits generated templates to voltage fluctuations; however, there is no definite constraint on the shape of the generated waveform. Therefore, the algorithm occasionally captures some clusters with characteristics that could not physically result from the action potential of a neuron. We manually labeled these clusters as noise in the templates-GUI based on the following criteria: 1) the cluster spread over many channels, 2) no peak and trough in the waveform shape, or the waveform has multiple peaks. Templates-GUI allows the splitting of clusters by cutting the spike in the PCS space. We used the splitting feature to remove the spikes far away from other spikes in each cluster. The number of discarded spikes in this step was always less than 10% of the spike within each cluster. We also visually inspected the clusters' autocorrelogram, and the cluster lacking a clear refractory period were labeled as multi-unit and were excluded from further analysis. After the manual curation of Kilosort results, the remaining clusters went through additional quality checks using ISI- violation, Presence ratio, and amplitude cut-off metrics [35,36]. The ISI violations metric determines refractory period violations, which indicate a unit containing spikes from multiple neurons. This metric quantifies the relative firing rate of contaminating spikes. To calculate the ISI violations, we counted the number of violations with intervals less than 1.5 ms, divided it by the potential violation time surrounding each spike, and normalized it by the overall spike rate. The resulting metric is always positive (or 0) and has no upper bound. We discarded clusters with a violation ratio of more than one [36]. We divided the experiment into 100 equal- sized blocks and estimated the presence ratio as the fraction of blocks, including one or more spikes from a specific unit. A low presence ratio indicates that the cluster either drifted out of the recording or could not be consistently tracked by Kilosort throughout the recordings [35]. The amplitude cut-off estimates a unit's false negative rate and serves as a missing ratio metric. To calculate this metric, we constructed a histogram of spike amplitudes. We then extracted the height of the histogram at the minimum amplitude and determined the percentage of spikes above the equivalent amplitude on the opposite side of the histogram peak. If the minimum amplitude matches the histogram peak, we set the missing ratio metric to 0.5, indicating a high likelihood that more than 50% of spikes are missing. It is important to note that this metric assumes a symmetrical distribution of amplitudes. We excluded the clusters with a missing ratio of more than 0.1 [35].

We calculated the orientation selectivity index (OSI) and direction selectivity index (DSI) using the as follow [37]:

$$OSI = \frac{\sqrt{(\sum R_i sin2\theta_i)^2 + (\sum R_i cos2\theta_i)^2}}{\sum R_i} \quad \text{Eq . 1}$$

Saeedi A, et al., J Radiol Clin Imaging 2024
DOI:10.26502/jrci.2809091

$$DSI = \frac{\sqrt{(\sum R_i sin\theta_i)^2 + (\sum R_i cos\theta_i)^2}}{\sum R_i} \quad \text{Eq . 2}$$

Where R_i is the response of the neuron to the drifting angle of θ_i. The figure panels were prepared using Adobe Illustrator.

Results

We recorded 103 V1 single units in 2 head-fixed mice. In mouse #1, we recorded spontaneous activities of 38 neurons for four weeks. In mouse #2, we recorded 65 neurons over ten weeks under passive viewing conditions. Firstly, we

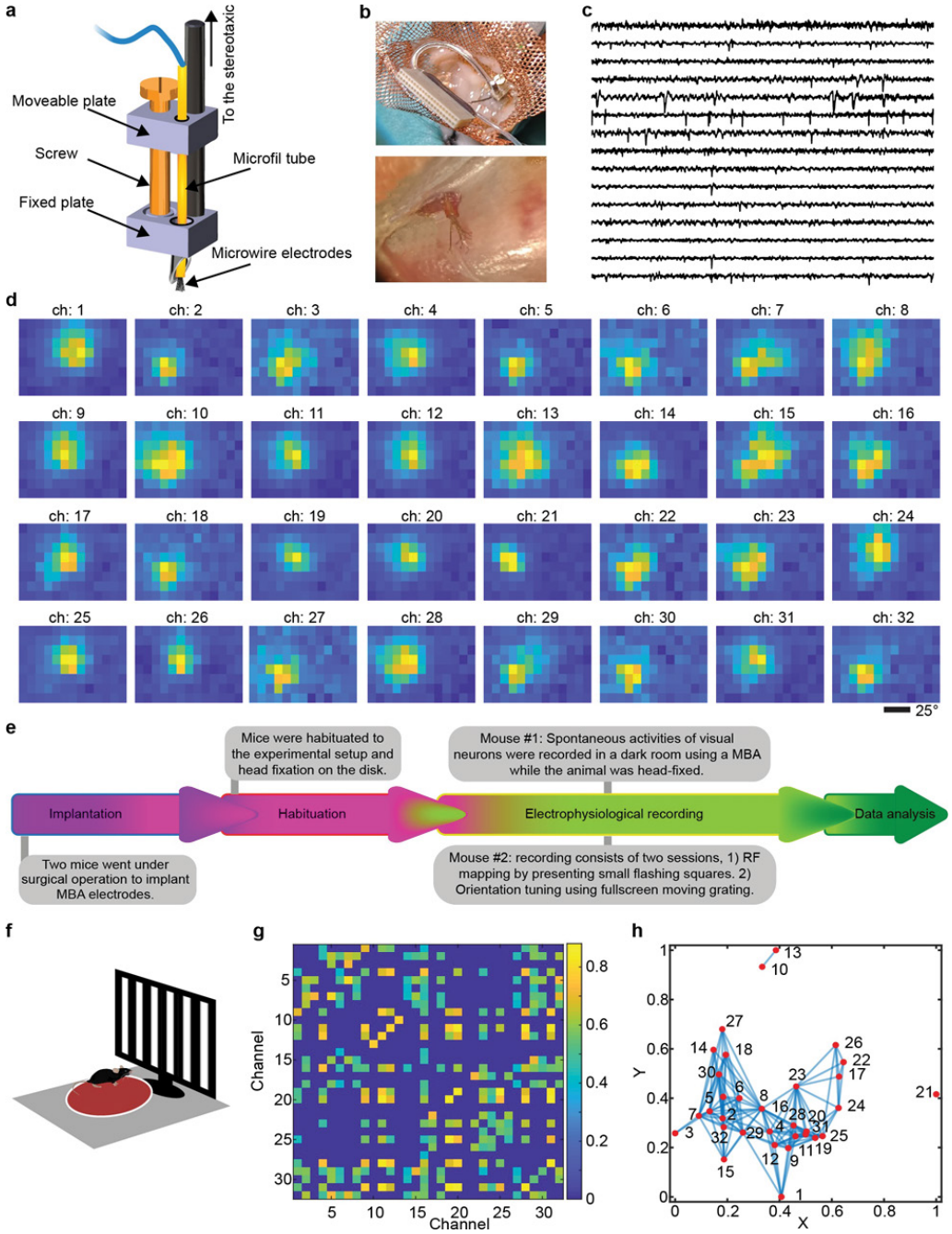

Figure 1: Technical consideration, RF mapping of single-day recording, and channel map estimation. a, Microwire brush array combined with an ultra-light microdrive. **b**, the upper panel shows the implanted electrode from the top; the lower panel shows the tip of the extracted electrode (16 channels) after mouse euthanasia. **c**, Example of high-pass filtered raw data. **d**, Receptive field of each channel estimated by the response of multi-unit signal to presented square at different locations on the monitor. **e**, this flowchart summarizes the experiment's procedure. **f**, The schematic figure shows the mouse on a disk for the recording session. During the electrophysiology recording, a full screen drifting grating was presented to mouse #2. **g**, correlation coefficient Matrix shows the cross-correlation of channels in the MUA band. Here, all the values lower than 2σ and diagonal elements are set to be zero only for better visualization. **h**, Estimated coordination of channels' tip (red dots) in a two-dimensional Euclidean plane. The links between dots indicate a correlation of more than 2σ in the MUA signal

Citation: Alireza Saeedi, Kun Wang, Nikos K. Logothetis, Masataka Watanabe. Longitudinal Single Neuron Electrophysiology in the Mouse Visual Cortex using Microwire Brush Arrays. Journal of Radiology and Clinical Imaging. 7 (2024): 09-19.

Saeedi A, et al., J Radiol Clin Imaging 2024
DOI:10.26502/jrci.2809091

conducted RF mapping to assess the RF center using the multi-unit response to presented black squares (15° widths) on a gray background at different locations selected in a pseudo-randomized manner from an 8 by 13 grid. Then, we recorded neuronal responses to full-screen drifting gratings in different directions from 0° to 315° with 45° steps.

Stable long-term recording of single unit activities:

We first confirmed the estimated channel map by inspecting the waveform shape of neurons in nearby channels. Figure 2a shows the captured waveform of three single units in nearby channels, and Figure 2b shows the auto-correlograms and cross-correlograms of these three single units. These results indicate well isolation of recorded neurons and an acceptable estimated channel map by the MDS method.

In order to confirm the stability of recordings, we calculated the number of recorded neurons per day. As shown in Figure 2c, the number of recorded neurons for mouse #1 remains the same over the recording period. However, for mouse #2, the number of recorded neurons increases in the first three weeks and remains the same for the rest of the recording period. Moreover, we calculated the duration in which every single neuron was tracked using MBA electrodes (Figure 2d). As it is shown in Figure 2d, 31% (n=12 from 38) of single

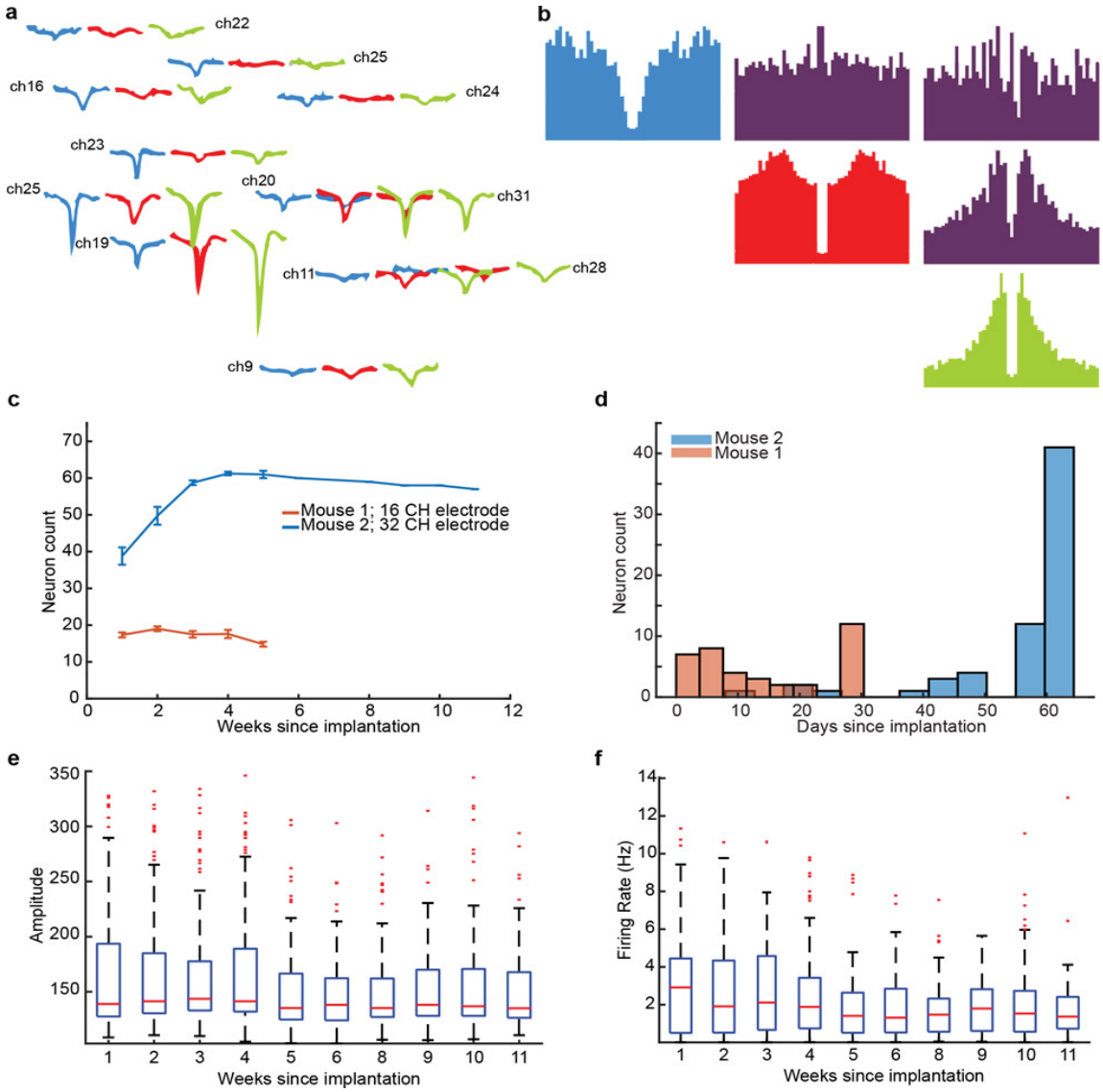

Figure 2: Stable long-term recording of single unit activities in mouse V1 using microwire brush electrode. a, The waveform of three example single units (blue, red, and green) in different nearby channels. Each row represents a channel and the recorded waveform of the example units in those channels are shown. **b**, The auto-correlograms (blue, red, and green) of the same single units as in panel a, and their cross-correlograms (purple). **c**, The average number of recorded neurons in each day of recording. Red shows the number of recorded neurons for mouse #1 with 16 channels. The blue line shows the recorded neurons from mouse #2. Error bars indicate the standard error of the mean. **d**, Histogram of neuron's life (the time we could track each neuron). **e**. and **f**, Waveform amplitudes and firing rates of recorded neurons, respectively. (n=65, mouse #2)

Saeedi A, et al., J Radiol Clin Imaging 2024
DOI:10.26502/jrci.2809091

units in mouse #1 and 63% (n=41 from 65) of single units in mouse #2 were detected by Kilosort for the whole period of recording. Furthermore, we calculated the amplitude and firing rate of the recorded neuron (Figure 2e and f). We find that the amplitude of recorded neurons remains stable during the recording period. However, we observed a slight change in the firing rate of neurons over time which might be related to neuronal plasticity in the brain and requires additional investigation [38]. These results indicate the potential of tracking single unit activity over a long time using microwire brush electrodes in mice.

The slight decline of the firing rate can also be explained by modulation of visual neurons by locomotion and behavioral state [39-41]. We performed passive recording where the mouse did not engage in any task. Therefore, due to the animal's lack of motivation and habituation to the setup, the animal spent more time in still condition on the disk, which may explain the decline of firing rate in the early weeks. However, we do not have the data of mouse running speed to evaluate this hypothesis, and it remains for future investigation. Raster and the PSTH of an example single unit. Plotting conventions are identical to Figure 3

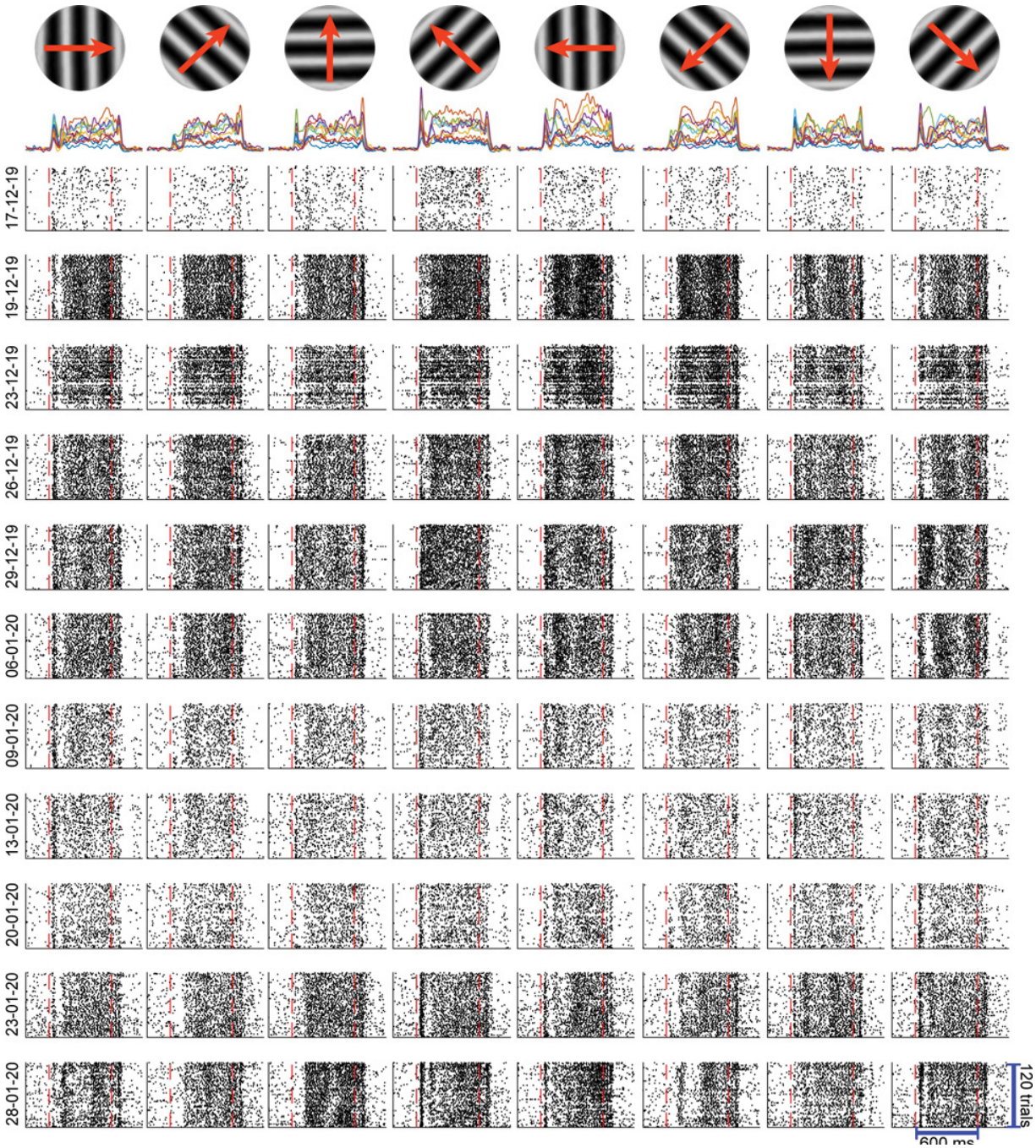

Figure 3: Example of single unit visual response.

Saeedi A, et al., J Radiol Clin Imaging 2024
DOI:10.26502/jrci.2809091

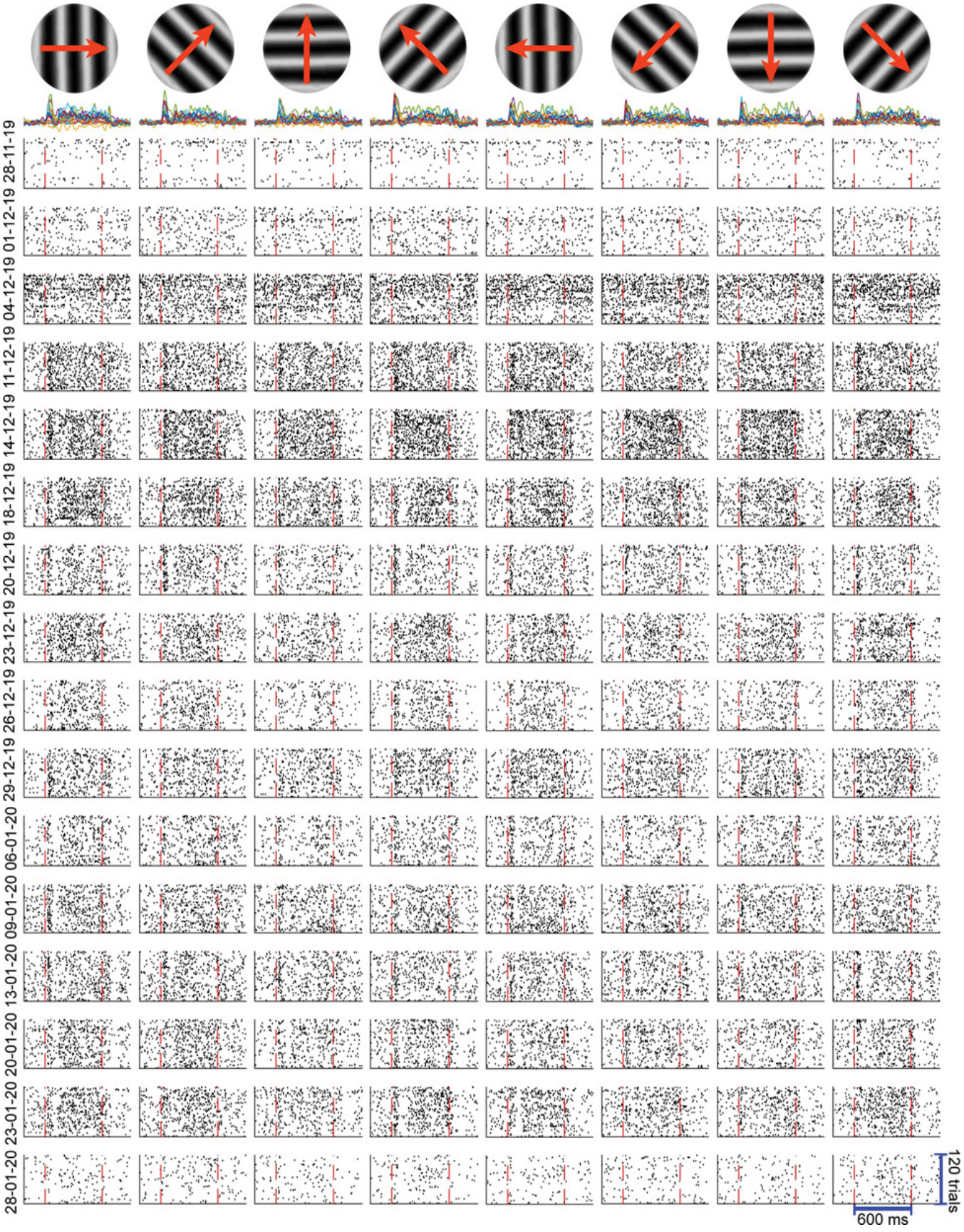

Figure 4: Example of single unit visual response.

Citation: Alireza Saeedi, Kun Wang, Nikos K. Logothetis, Masataka Watanabe. Longitudinal Single Neuron Electrophysiology in the Mouse Visual Cortex using Microwire Brush Arrays. Journal of Radiology and Clinical Imaging. 7 (2024): 09-19.

Saeedi A, et al., J Radiol Clin Imaging 2024
DOI:10.26502/jrci.2809091

Long-term stability of visual selectivity in mouse V1

In order to investigate the long-term stability of functional properties of visual neurons, we presented mouse #2 with full screen drifting grating in 8 different moving directions. Figure 3 and Figure 4 show the raster and peri-stimulus time histogram (PSTH) of two example neurons in response to the different drifting grating. This suggests the long-term stability of visual responses in mouse V1. To further investigate the functional stability of visual neurons, we calculated the average response of each neuron to different moving directions and captured the direction tuning curve of neurons for each day of recording. Figure5 a-c shows the tuning curve of three example neurons in which the neuron in panel a shows a direction-selective neuron while the other two in panels b and c exhibit orientation-selective behavior. Next, we calculated OSI and DSI using Eq. 1 and Eq. 2. As shown in Figure 5d and e, OSI and DSI exhibit stability throughout the recording (i. e., ten weeks). Next, we captured the preferred angle of each neuron as the angle which maximally evokes the neuron. We calculated the day-to-day difference preferred for single units in which their OSI was larger than the mean OSI of the population (OSI>0.188, n= 39) to further confirm the stability

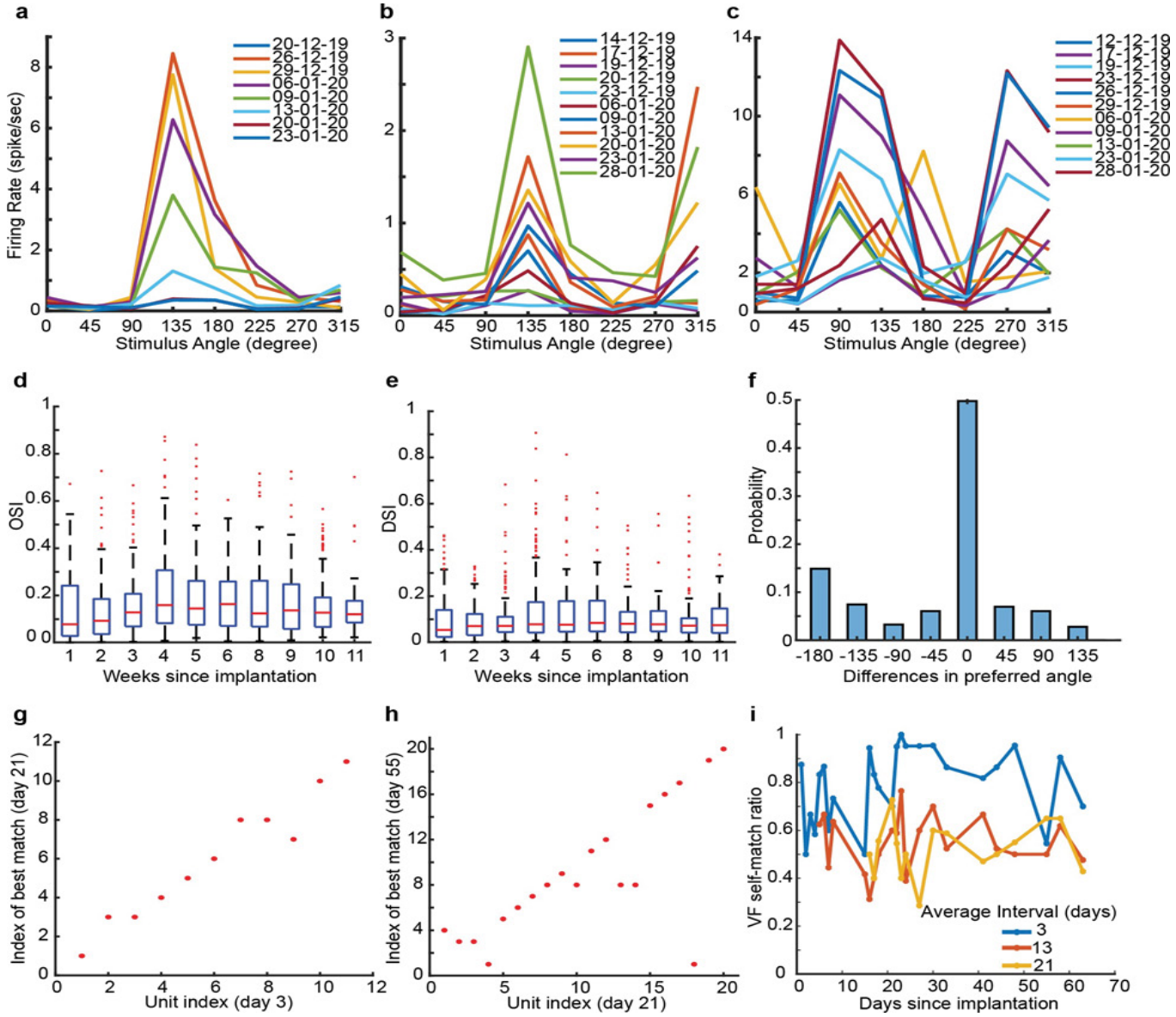

Figure 5: Stability of OSI and DSI in mouse visual cortex.

a-c, Direction tuning curve of three example neurons over different days of recording. **d and e**, Respectively, OSI and DSI of 132 recorded neurons in mouse #**2. f,** The probability distribution of day-to-day changes of preferred angle for selective units (OSI>0.186, n=39). **g and h,** Scatter plots show the index of units against the index of best-matched units on the next session with intervals of 18 and 34 days, respectively. **i**, The ratio of self-matched VF is plotted over time with different average intervals of matching comparison. Here we report only the average comparison intervals, as the recordings were not performed with daily intervals.

of visual responses. As shown in Figure 5f, the probability of differences in preferred angle is mostly zero and remains under 0.1 for all other values except -180. This 180 of change is due to a slight change in response to the same orientation but the different moving direction of drifting grating in orientation-selective neurons. These results indicate OSI's and DSI's long-term stability in the mouse visual cortex. After confirming the stability of visual response properties, we aimed to determine whether a group of spikes recorded across different days corresponded to the same neuron. We based our analysis on the distinct visual responses of neurons in the primary visual cortex compared to their neighboring neurons [32,42-44]. We calculated a visual fingerprint (VF) for the orientation-selective neurons based on their response profile to eight drifting grating of different directions and their average PSTH responses. We then checked if every single unit's VF matches its own VF or other single units on consecutive days. Figure 5 g and h show examples of best-matched indices of recorded single units after an interval of 18 and 34 days. We observed that the majority of units can be tracked over time. To quantify this effect, we calculated the ratio of self-matched VF of recorded single units over time with an average interval of 3, 13, and 21 days (Figure 5i). We found that, on average, the VF of 79.4, 54.54, and 52.20 % of the well-isolated single units were best matched to their own VF after an average of 3, 13, and 21 days interval.

Discussion

Our results show the feasibility of long-term stable electrophysiology in mice using MBA probes. MBA probes are suitable for robust long-term recording of single units' activities in longitudinal in-vivo studies of brain functions [7,9]. Here we deployed an ultra-light microdrive combined with MBA probes to track the activities of single units in the mouse visual cortex. The combination of the MBA probe with ultra-light microdrive provides the opportunity for very slow advancement of the probe into the mouse brain tissue and prevents the over bending of wires used in monkey studies [7]. Moreover, moving electrodes allow recording from fresh brain tissue in case of a decline in the signal quality [45]. To reconstruct the organization of wires in the brain and infer the channel map of recording sites, we applied the MDS method [30] to the MUA signal and used the resulting channel map for spike sorting of firing neurons using the Kilosort algorithm [29]. Furthermore, we concatenated all the recorded data over different recording days and fed them into Kilosort to accurately track single units' activity over a long term (i.e., ten weeks). Using our method, 35% of visually evoked neurons have been tracked for the whole recording period. The number of recorded neurons and their magnitude remained stable; however, the firing rate of neurons changed slightly on different days, which can be due to the state of the animal or neuronal plasticity in the brain and requires further investigation [38]. The brain's functional properties are routinely measured over short periods, which is not comparable to the lifespan of neurons. Several studies chronically tracked the activities of individual single-units in different brain regions to assess the variability of neuronal function versus their stability [38]. It has been shown that visual neurons in monkeys' inferotemporal cortex maintain their selectivity to complex visual patterns such as objects and faces [46,47]. An interventional imaging study in mice has shown that visual tuning properties are robust to monocular deprivation [48]. However, how the neuronal function in the primary visual cortex change over an extended timescale remains unclear. Here we demonstrate that the orientation and direction selectivity of mice V1 neurons remain constant over months. The importance of larger sample sizes in animal studies for ensuring statistical power and the generalizability of the findings cannot be overstated. Studies with larger cohorts provide robust and conclusive results, for instance, Steinmetz et al. (2021),Schoonover et al. (2021), and Chung et al. (2019), which explored the quality and stability of silicon probe and polymer electrode arrays for chronic recordings of single units' activities, employed sample sizes ranging from 3 to 6 animals [32,49,50]. These studies highlight the benefits of larger sample sizes in elucidating important aspects of the experimental setup. Although our study was confined to two animals, we believe this study benefits the field. Nevertheless, we recognize the significance of larger sample sizes for future investigations in this field. The current study employed different recording procedures for the two mice. One mouse was implanted with a 16-channel MBA and recorded over four weeks without visual stimulation. In contrast, the other mouse underwent recordings over ten weeks using a 32-channel MBA and was presented with visual stimuli. By using these distinct recording protocols, we demonstrated the versatility of our developed method in capturing neural activity both in the absence and presence of external stimulation and the possibility of increasing the number of electrodes and elongating the experiment duration. Our results prove proof-of-concept that MBA can be used in different experimental paradigms to investigate brain function. The development of implantable and movable microelectrodes with large-number recording channels is critical for studying brain functions at the cellular level. Moreover, achieving stable neuronal signals over a long period is necessary for longitudinal studies. Although the current study targets the visual cortex to record from, the technique provided here can be used to record brain activities from different cortical areas. Moreover, the long travel distance (6mm) provided by the microdrive allows recording from deep brain structures. Our results showcase using MBA probes combined with an ultra-lightweight microdrive in mice. Such a combination equips the big community of electrophysiologists using small animals (e.g., mice) with a proper tool to tackle different questions. For instance, by performing long-term recordings in the visual cortex, we can gain insights into the stability and

plasticity of neural representations over time and examine the impact of sensory experience on cortical activity.

Data and Code Availability

Raw data and the codes are available upon request.

Competing Interest Statement

The authors have no competing interests to disclose.

Funding

This work was funded by the Max Planck Society.

Authors Contributions

Conceptualization – MW; Data acquisition and curation – AS, KW; Formal analysis – AS, MW; Methodology – AS,

MW; Project administration – MW; Supervision – MW; Visualization – AS, MW; Writing – AS, MW; Resources NKL.

References

1. Campbell PK, Jones KE, Huber R.J, et al. A silicon-based, three- dimensional neural interface: manufacturing processes for an intracortical electrode array. IEEE Tran Biomed Eng 38 (1991): 758-768.
2. Gray C M, Maldonado PE, Wilson M, et al. Tetrodes markedly improve the reliability and yield of multiple single-unit isolation from multi-unit recordings in cat striate cortex. J Neurosci Methods 63 (1995): 43-54.
3. Csicsvari J, Henze DA, Jamieson B, et al. Massively parallel recording of unit and local field potentials with silicon-based electrodes. J Neurophysiol 90 (2003): 1314-1323.
4. Nicolelis M A, Dimitrov D, Carmena JM, et al. Chronic, multisite, multielectrode recordings in macaque monkeys. Pro Natl Acad Sci U S A 100 (2003): 11041-11046.
5. Buzsáki G. Large-scale recording of neuronal ensembles. Nature Neurosci 7 (2004): 446-451.
6. Wise KD, Anderson DJ, Hetke JF, et al. Wireless implantable microsystems: high-density electronic interfaces to the nervous system. Proc IEEE 92 (2004): 76-97.
7. McMahon DB, Bondar IV, Afuwape OA, et al. One month in the life of a neuron: longitudinal single-unit electrophysiology in the monkey visual system. J Neurophysiol 112 (2014): 1748-1762.
8. Jun JJ, Steinmetz N A, Siegle JH, et al. Fully integrated silicon probes for high-density recording of neural activity. Nat 551 (2017): 232-236.
9. Guan S, Wang J, Gu X, et al. Elastocapillary self-assembled neurotassels for stable neural activity recordings. Sci Adv 5 (2019): eaav2842.
10. Rousche PJ, & Normann RA. Chronic recording capability of the Utah Intracortical Electrode Array in cat sensory cortex. J Neurosci Methods 82 (1998): 1-15.
11. Williams JC, Rennaker RL, & Kipke DR. Long-term neural recording characteristics of wire microelectrode arrays implanted in cerebral cortex. Brain Res Pro 4 (1999): 303-313.
12. Biran R., Martin D C, Tresco P A. Neuronal cell loss accompanies the brain tissue response to chronically implanted silicon microelectrode arrays. Exp Neurol 195 (2005): 115-126.
13. Polikov VS, Tresco PA, Reichert WM. Response of brain tissue to chronically implanted neural electrodes. J Neurosci Methods 148 (2005): 1-18.
14. Gilletti A, & Muthuswamy J. Brain micromotion around implants in the rodent somatosensory cortex. J Neural Eng 3 (2006): 189.
15. McConnell G C, Rees HD, Levey A I, et al. Implanted neural electrodes cause chronic, local inflammation that is correlated with local neurodegeneration. J Neural Eng 6 (2009): 056003.
16. Rousche P J, Pellinen DS, Pivin D P, et al. Flexible polyimide-based intracortical electrode arrays with bioactive capability. IEEE Trans Biomed Eng 48 (2001): 361-371.
17. Kozai T D Y, Langhals N B, Patel P R., et al. Ultrasmall implantable composite microelectrodes with bioactive surfaces for chronic neural interfaces. Nat Mater 11 (2012): 1065-1073.
18. Tian B, Liu J, Dvir T, et al. Macroporous nanowire nanoelectronic scaffolds for synthetic tissues. Nat Mater 11 (2012): 986-994.
19. Guitchounts G, Markowitz JE, Liberti W A, et al. A carbon-fiber electrode array for long-term neural recording. J Neural Eng 10 (2013): 046016.
20. Kim D.-H, Viventi J, Amsden J J, et al. Dissolvable films of silk fibroin for ultrathin conformal bio-integrated electronics. Nat Mater 9 (2010): 511-517.
21. Kim T.-i, McCall JG, Jung YH, et al. Injectable, cellular-scale optoelectronics with applications for wireless optogenetics. Sci 340 (2013): 211-216.
22. Nguyen J K, Park DJ, Skousen J L, et al. Mechanically-compliant intracortical implants reduce the neuroinflammatory response. J Neural Eng 11 (2014): 056014.
23. Khodagholy D, Gelinas JN, Thesen T, et al. NeuroGrid: recording action potentials from the surface of the brain. Nat Neurosci 18 (2015): 310-315.

24. Canales A, Jia X, Froriep UP, et al. Multifunctional fibers for simultaneous optical, electrical and chemical interrogation of neural circuits in vivo. Nat Biotech 33 (2015): 277-284.

25. Liu J, Fu T.-M, Cheng Z, et al. Syringe-injectable electronics. Nat Nanotech 10 (2015): 629-636.

26. Xie C, Liu J, Fu T.-M, et al. Three-dimensional macroporous nanoelectronic networks as minimally invasive brain probes. Nat Mater 14 (2015): 1286 1292.

27. Luan L, Wei X, Zhao Z, et al. Ultraflexible nanoelectronic probes form reliable, glial scar–free neural integration. Sci Adv 3 (2017): e1601966.

28. Lind G, Linsmeier C E, Thelin J, et al. Gelatine-embedded electrodes—a novel biocompatible vehicle allowing implantation of highly flexible microelectrodes. J Neural Eng 7 (2010): 046005.

29. Pachitariu M, Steinmetz N, Kadir S, et al. Kilosort: realtime spike-sorting for extracellular electrophysiology with hundreds of channels. BioRxiv (2016).

30. Mead A. Review of the development of multidimensional scaling methods. J Royal Statistical Soci 41 (1992): 27-39.

31. Pachitariu M, Steinmetz N A, Kadir SN, et al. Fast and accurate spike sorting of high-channel count probes with KiloSort. Adv Neural Informat Proc Syst 29 (2016).

32. Steinmetz N A, Aydin C, Lebedeva A, et al. Neuropixels 2.0: A miniaturized high-density probe for stable, long-term brain recordings. Sci 372 (2021): eabf4588.

33. Rossant C, Kadir SN, Goodman D F, et al. Spike sorting for large, dense electrode arrays. Nat Neurosci 19 (2016): 634-641.

34. Lenzi S S, Nick. phy-contrib.template-gui module (2018). In https://github.com/kwikteam/phy-contrib/.

35. Siegle J H, Jia X, Durand S, et al. Survey of spiking in the mouse visual system reveals functional hierarchy. Nat, 592 (2021): 86-92.

36. Hill D N, Mehta SB & Kleinfeld D. Quality metrics to accompany spike sorting of extracellular signals. J Neurosci 31 (2011): 8699-8705.

37. Wilson D E, Whitney DE, Scholl B, et al. Orientation selectivity and the functional clustering of synaptic inputs in primary visual cortex. Nat Neurosci 19 (2016): 1003-1009.

38. Clopath C, Bonhoeffer T, Hübener M, et al. Variance and invariance of neuronal long- term representations. Philosophical Transactions of the Royal Society B: Biol Sci 372 (2017): 20160161.

39. Niell, C.M. and M.P. Stryker, Highly selective receptive fields in mouse visual cortex. Journal of Neuroscience, 2008. 28(30): p. 7520-7536.

40. Dadarlat, M.C. and M.P. Stryker, Locomotion enhances neural encoding of visual stimuli in mouse V1. Journal of Neuroscience, 2017. 37(14): p. 3764-3775.

41. Niell, C.M. and M.P. Stryker, Modulation of visual responses by behavioral state in mouse visual cortex. Neuron, 2010. 65(4): p. 472-479. Kampa BM, Roth MM, Göbel W, et al. Representation of visual scenes by local neuronal populations in layer 2/3 of mouse visual cortex. Front Neural Circuits 5 (2011): 18.

42. Kampa BM, Morgane MR, Werner G, et al., Representation of visual scenes by local neuronal populations in layer 2/3 of mouse visual cortex. Frontiers in neural circuits 5 (2011): 18.

43. Bonin V, Histed M H, Yurgenson S, et al. Local diversity and fine-scale organization of receptive fields in mouse visual cortex. J Neurosci 31 (2011): 18506-18521.

44. Ohki K, Chung S, Ch'ng Y H, et al. Functional imaging with cellular resolution reveals precise micro-architecture in visual cortex. Nat 433 (2005): 597-603.

45. Galashan F O, Rempel HC, Meyer A, et al. A new type of recording chamber with an easy-to-exchange microdrive array for chronic recordings in macaque monkeys. J Neurophysiol 105 (2011): 3092-3105.

46. Bondar IV, Leopold DA, Richmond BJ, et al. Long-term stability of visual pattern selective responses of monkey temporal lobe neurons. PloS one 4 (2009): e8222.

47. McMahon DB, Jones AP, Bondar I V, et al. Face-selective neurons maintain consistent visual responses across months. Proc Nat Acad Sci 111 (2014): 8251-8256.

48. Rose T, Jaepel J, Hübener M, et al. Cell-specific restoration of stimulus preference after monocular deprivation in the visual cortex. Sci 352 (2016): 1319-1322.

49. Chung JE, Hannah RJ, Jiang LF, et al., High-density, long-lasting, and multi-region electrophysiological recordings using polymer electrode arrays. Neuron, 101 (2019): 21-31

50. Schoonover, C.E., Sarah NO, Richard A, et al., Representational drift in primary olfactory cortex. Nature, 2021. 594 (7864): 541-546.